Molecular Cell, Vol. 15, 279–286, July 23, 2004, Copyright ©2004 by Cell Press

A Glutamine Switch Mechanism for Nucleotide Selectivity by Phosphodiesterases

Short Article

Kam Y.J. Zhang, Graeme L. Card, Yoshihisa Suzuki, D. Richard Artis, Daniel Fong, Sam Gillette, Davin Hsieh, Joshua Neiman, Brian L. West, Chao Zhang, Michael V. Milburn, Sung-Hou Kim,[1] Joseph Schlessinger,[2] and Gideon Bollag*
Plexxikon Inc.
91 Bolivar Drive
Berkeley, California 94710
[1]Department of Pharmacology
Yale University School of Medicine
333 Cedar Street
New Haven, Connecticut 06520
[2]220 Calvin Laboratory
University of California, Berkeley
Berkeley, California 94720

Summary

Phosphodiesterases (PDEs) comprise a family of enzymes that modulate the immune response, inflammation, and memory, among many other functions. There are three types of PDEs: cAMP-specific, cGMP-specific, and dual-specific. Here we describe the mechanism of nucleotide selectivity on the basis of high-resolution co-crystal structures of the cAMP-specific PDE4B and PDE4D with AMP, the cGMP-specific PDE5A with GMP, and the apo-structure of the dual-specific PDE1B. These structures show that an invariant glutamine functions as the key specificity determinant by a "glutamine switch" mechanism for recognizing the purine moiety in cAMP or cGMP. The surrounding residues anchor the glutamine residue in different orientations for cAMP and for cGMP. The PDE1B structure shows that in dual-specific PDEs a key histidine residue may enable the invariant glutamine to toggle between cAMP and cGMP. The structural understanding of nucleotide binding enables the design of new PDE inhibitors that may treat diseases in which cyclic nucleotides play a critical role.

Introduction

Cyclic nucleotide phosphodiesterases (PDEs) are enzymes that control the level of the cyclic nucleotides, cAMP and cGMP, two second messengers that regulate a great variety of important physiological processes. For example, many G protein-coupled receptors mediate their cellular responses by controlling the level of cyclic nucleotide production (Pierce et al., 2002). In addition, another important second messenger, nitric oxide, which is generated in response to a variety of extracellular stimuli, activates guanylate cyclase, resulting in elevation of cGMP that in turn activates cGMP-dependent intracellular signaling pathways (Corbin and Francis, 1999). Clearly, the genesis of nucleotide selectivity of these enzymes involved in cyclic nucleotide metabolism is important for diverse aspects of cellular physiology, including the immune response, neuronal activity, hypertension, and the inflammatory response. Consequently, the development of specific inhibitors of PDE isoforms will enable the development of new drugs for the treatment of a wide variety of diseases. Indeed, PDE5 inhibitors such as Viagra have been applied for the treatment of erectile dysfunction (Corbin and Francis, 1999) and PDE4 inhibitors such as Rolipram have potent anti-inflammatory properties (Conti et al., 2003).

The 21 genes encoding human PDEs can be grouped into enzymes selective toward cAMP, cGMP, or both cyclic nucleotides. One group of PDEs selectively hydrolyzes cAMP (PDE4ABCD, PDE7AB, and PDE8AB), a second group of enzymes is selective toward cGMP (PDE5A, PDE6ABC, and PDE9A), and the remaining enzymes hydrolyze both cAMP and cGMP (PDE1ABC, PDE2A, PDE3AB, PDE10A, and PDE11A) (Beavo and Brunton, 2002; Conti, 2000; Mehats et al., 2002). In addition to the multiple genes that code for these enzymes, PDE diversity is further increased by alternative RNA processing and multiple promoters that result in the formation of many PDE isoforms. All PDEs contain a conserved catalytic domain of approximately 270 amino acids (18%–46% sequence identity; see Supplemental Figure S1 at http://www.molecule.org/cgi/content/full/15/2/279/DC1) at the carboxyl terminus. Regulatory domain(s) that vary widely among the PDE classes flank the catalytic core and include regions that autoinhibit the catalytic domains as well as targeting sequences that control subcellular localization (Houslay and Adams, 2003; Sonnenburg et al., 1995).

The crystal structures of the catalytic domains of PDE4B, PDE4D, and PDE5A (Huai et al., 2003a, 2003b, 2004; Lee et al., 2002; Sung et al., 2003; Xu et al., 2000, 2004) have shown that catalytic domains adopt a compact α-helical structure consisting of 16 α-helices that can be divided into three subdomains (Xu et al., 2000). A deep hydrophobic pocket is formed at the interface of the three subdomains, and a tightly bound zinc ion is found at one end of this pocket. It has been proposed that an invariant glutamine residue plays an important role in PDE nucleotide selectivity (Xu et al., 2000, 2004). However, the precise mechanism by which the glutamine determines cAMP, cGMP, and dual specificity in the three groups of PDEs has remained unclear.

In this report we describe the high-resolution three-dimensional crystal structures of PDE4B and PDE4D in complex with AMP, the structure of chimeric PDE5A, herein referred to as PDE5A, in complex with GMP, and the apo-structure of the dual-specific enzyme PDE1B. These structures reveal a glutamine switch mechanism for the control of PDE selectivity toward cyclic nucleotides. Specifically, an invariant glutamine residue in the active site of the enzyme can alternatively adopt two different orientations: in one orientation the hydrogen bond (H-bond) network supports guanine binding leading to cGMP selectivity and in the other orientation the network supports adenine binding resulting in selectivity toward cAMP. We propose that in dual-specific PDEs

*Correspondence: gbollag@plexxikon.com

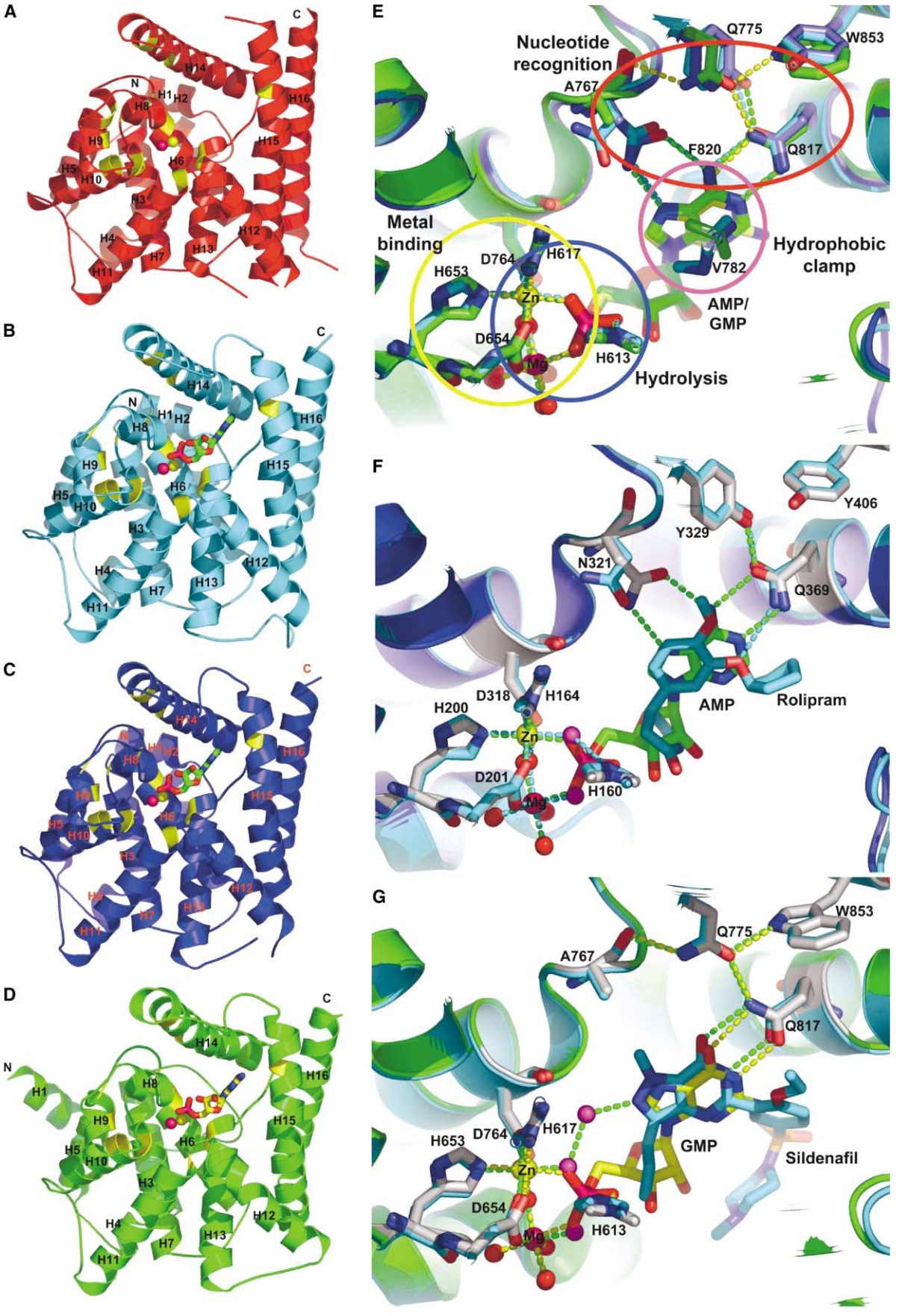
A
B
C
D
E
F
G
N
C
H1
H2
H3
H4
H5
H6
H7
H8
H9
H10
H11
H12
H13
H14
H15
H16
Nucleotide recognition
Q775
W853
A767
F820
Q817
Metal binding
Hydrophobic clamp
V782
D764
H617
H653
Zn
AMP/ GMP
D654
H613
Mg
Hydrolysis
Y406
Y329
N321
Q369
D318
H164
H200
AMP
Rolipram
D201
H160
GMP
Sildenafil

the orientation of the key glutamine residue switches between the two orientations resulting in dual specificity toward cyclic nucleotides. This glutamine residue thus provides a switch to control the selectivity of PDEs to cAMP, cGMP, or toward both cyclic nucleotides. Our structures also reveal a "hydrophobic clamp" that holds the purine base tightly in the active site and thereby contributes significantly to the energy of nucleotide and inhibitor binding.

Results and Discussion

Description of Crystal Structures of PDEs and Their Nucleotide Complexes

In order to elucidate the molecular basis underlying the selectivity of PDEs toward cyclic nucleotides, we have determined high-resolution crystal structures of the cAMP-specific enzymes PDE4B and PDE4D in complex with AMP and the crystal structure of the cGMP-specific enzyme PDE5A in complex with GMP. We have also determined a high-resolution crystal structure of the dual-specific enzyme PDE1B. These crystal structures show that the overall topology is highly conserved among the three classes of PDEs. All four PDEs adopt a compact α-helical structure (Figure 1) consisting of three subdomains. A deep hydrophobic pocket is formed at the interface of the three subdomains. Among the 17 amino acids invariant across all 21 PDE gene family members, 12 amino acids lie within this conserved pocket and the other five amino acids are nearby (Figure 1).

PDE1B contains a long sequence insertion compared to other PDEs in this study (Supplemental Figure S1), occurring in the loop connecting helices 15 and 16 (residues K442-V479). This loop region is mostly disordered except for residues 442-449 and 476-479, but has little impact on the overall structure of PDE1B, which has an RMSD of 1.77 Å to PDE4B. Consequently, residues S454 to V471 in this region can be deleted to produce crystals with improved diffraction quality without affecting the overall structure and enzymatic activity.

The structure of wild-type apo PDE5A (not shown) has a loop (L672 to H685) that differs dramatically from that of other PDEs. This loop extends into the active site and blocks substrate and inhibitor binding. The corresponding residues L293 to H307 in PDE4B form helix α9 and part of helix α10. This region adopts an α-helical conformation in all the other PDEs. In co-crystal structures of PDE5A complexed with Sildenafil (Viagra), Vardenafil (Levitra), and Tadalafil (Cialis), this loop region extends out and caps the active site upon inhibitor binding (Sung et al., 2003), providing further evidence for the conformational flexibility of this loop. In our apo-structure, the Mg in the active site has been displaced by a phosphate ion from the crystallization buffer. The conformation of the loop and the binding of phosphate in the active site prohibit substrate and inhibitor binding. In order to overcome these crystallographic challenges, we have prepared a mutant PDE5A protein in which this loop has been replaced with the corresponding region from PDE4B. The swapped region from PDE4B adopts the same conformation in the PDE5A mutant protein as in PDE4B, and it has no impact on the rest of the PDE5A structure. Moreover, the chimeric PDE5A protein exhibits similar activity as wild-type PDE5A toward its natural substrate cGMP (data not shown).

The products of the hydrolytic reaction, AMP and GMP, bind in an extended *anti* conformation at the active site of their respective catalytic enzyme. The phosphate, ribose, and purine base from three independently determined co-crystal structures, PDE4D+AMP, PDE4B+AMP, and PDE5A+GMP, superimpose very well (Figure 1E). Analysis of the PDE active site reveals four key interactions that affect cyclic nucleotide selectivity and catalysis: (1) metal binding; (2) coordination to the phosphate group; (3) a hydrophobic "clamp" that affords affinity; and (4) a hydrogen-bonding network that determines nucleotide selectivity (Figure 1E). The ribose has a C3′-endo puckering configuration and is surrounded by hydrophobic residues L725, L765, and F786 in PDE5A. The hydroxyl groups of the ribose ring are H-bonded with nearby water molecules, but the ribose makes no H-bonds to any amino acid. The purine base is held tightly in the active site by a "hydrophobic clamp" formed by F820 and V782 on each side and additional hydrophobic interactions with F786 and I768 in PDE5A. The binding of AMP to PDE4D displaces the two water molecules (W4 and W6) that were part of the metal coordination sphere in PDE4D as observed in the PDE4D+Rolipram complex (Figure 1F). Similarly, the binding of GMP to PDE5A displaces the same two water molecules (W4 and W6) that were part of the metal coordination sphere in PDE5A as seen in the PDE5A+Sildenafil complex (Figure 1G). The evolutionarily optimized substrate binding pocket and its constituent residues can be further exploited for the design of inhibitors with favorable binding characteristics. For example, the pyrazolopyrimidinone group of sildenafil mimics that of guanine in cGMP and has the same H-bond donor and acceptor features to form a

Figure 1. Crystal Structures of PDE1B, PDE4B, PDE4D, and PDE5A in Complex with AMP or GMP

The overall structures of PDE1B, PDE4B, PDE4D, and PDE5A are represented by ribbon diagrams colored red, cyan, blue, and green, respectively. Zinc and magnesium ions are represented by yellow and magenta spheres, respectively. This color scheme is used throughout the figures of this report. (A)–(D) have the same view looking down the nucleotide binding pocket for ready comparison. The sixteen helices are labeled in all four PDEs. In each case, positions of all 17 invariant residues are highlighted in yellow. (E)–(G) have the same zoom-in view of the active site. (A) PDE1B apo-structure. (B) PDE4B in complex with AMP. Conventional atomic color coding is used to represent AMP except carbon atoms are colored green. (C) PDE4D in complex with AMP. (D) PDE5A chimera in complex with GMP. Conventional atomic color coding is used to represent GMP except carbon atoms are colored yellow. (E) Superposition of PDE4B+AMP, PDE4D+AMP, and PDE5A+GMP show conserved binding mode of nucleotides. The PDE nucleotide binding site can be divided into four regions: nucleotide recognition, hydrophobic clamp, metal binding, and hydrolysis. (F) Overlay of PDE4D with AMP or Rolipram reveals conserved binding interactions. (G) Overlay of PDE5A with GMP or Sildenafil reveals conserved binding interactions. The pyrazolopyrimidinone group of Sildenafil mimics the guanine in GMP and they overlap in space. They both are sandwiched by the hydrophobic clamp and also make the same bidentate H-bonds with the conserved Q817.

bidentate H-bond with Q817 with its amide orientation evolved to bind cGMP.

A Glutamine Switch Mechanism for Nucleotide Selectivity

Comparison of the high-resolution co-crystal structures of AMP-bound PDE4B and PDE4D, the GMP-bound PDE5A, and apo-PDE1B reveals that the orientation of the γ-amide group of the glutamine residue plays a critical role in nucleotide recognition and selectivity. This glutamine switch mechanism is controlled by an intricate network of hydrogen bonds near the conserved glutamine, providing a molecular mechanism for selectivity toward cAMP, cGMP, or both cyclic nucleotides.

In the co-crystal structure of PDE4D complexed with AMP (Figure 2A), the absolutely conserved Q369 forms a bidentate H-bond with the adenine moiety. Specifically, the Nε atom of Q369 donates an H-bond to the N1 atom of the adenine ring and the Oε accepts a H-bond from N6 in the exocyclic amino group of adenine. This orientation of Q369 is stabilized by H-bonding of Oε to the phenolic hydroxyl group Oη of Y329. The adenine ring also forms a bidentate H-bond with N321 in PDE4D: N321 donates one H-bond from Nδ to N7 of the adenine ring and accepts one H-bond from the N6 of the exocyclic amino group to its Oδ. From our co-crystal structure of PDE4D with rolipram, we noticed that this N321 has adopted a different conformation that would be distal to the adenine ring (Figure 1F). Since there are no inherent interactions that lock this N321 in place, the interaction of N321 with AMP is probably a consequence of, rather than a determinant of, nucleotide binding. The co-crystal structure of AMP bound to PDE4B is almost identical to that of AMP bound to PDE4D indicating that the mode of nucleotide recognition discussed above is also applicable to other PDE4 isoforms.

By contrast, in the co-crystal structure of GMP bound to PDE5A, the orientation of the key glutamine (Q817 in PDE5) is switched from that in PDE4D to allow H-bonding specific to the guanine ring of 5′-GMP (Figure 2B): Oε accepts an H-bond from N1 in the guanine ring and Nε donates an H-bond to the exocyclic O6 atom of guanine. This orientation of Q817 is constrained by the H-bond between its Nε atom and the Oε atom of Q775. The orientation of Q775 is in turn determined by the two H-bonds that it forms with A767 and W853 where the Nε atom of Q775 donates a H-bond to the backbone carbonyl of A767 and the Oε atom of Q775 accepts an H-bond from the Nε of W853. This intricate network of H-bond determines the orientation of the γ-amide group of Q817 that is favorable for cGMP but unfavorable for cAMP binding in PDE5.

PDE1B is an example of an enzyme that catalyzes hydrolysis of either cAMP or cGMP. The active site of PDE1B is shown with a model of bound 5′-AMP (Figure 2C) or 5′-GMP (Figure 2D). The key glutamine, in this case Q421, may be able to adopt both of the orientations observed in the PDE4 and PDE5 structures, since there is no H-bond network to constrain the orientation of its γ-amide group in this enzyme. The rotational flexibility of the γ-amide group of Q421 in PDE1B is also reflected through its relatively higher thermal motion in the crystal structure as revealed from the analysis and comparison of the temperature factors. Moreover, the other two key residues involved in the H-bond network that determines the Q-switch (Q775 and A767 in PDE5A; N321 and Y329 in PDE4D) are analogous to H373 and H381 in PDE1B (Supplemental Table S1). Therefore, the binding of either cAMP or cGMP can be accommodated by the H-bonding flexibility of these two histidine residues, H373 and H381.

The mechanism proposed in this report for the control of PDE selectivity can be extrapolated beyond the PDEs whose structures are presented. Additional selectivity determinants are defined by three residues positioned near the key glutamine residue, and these are compared among all 21 human PDEs in Table 1 (Supplemental Data). An asparagine (N395 in PDE4B) that makes key hydrogen bonds with adenine is conserved in all the cAMP-specific PDEs (PDE4, PDE7, PDE8). Interestingly, this residue is also found in the cGMP-specific PDE9; the orientation would most likely be switched. Similarly, the neighboring residues that anchor the key glutamine orientation (Q775, A767, and W853 in PDE5A) are all conserved in the cGMP-specific PDEs, with PDE9 as an exception (Supplemental Table S1).

In order to confirm the importance of these residues in nucleotide recognition, the residues corresponding to "Position 1," "Position 2," and "Position 3" (Supplemental Table S1) were mutated: the residues of PDE4B were mutated to the corresponding residues of PDE5 (4AQW: PDE4B with N395A, Y403Q, Y480W) or PDE1B (4HH: PDE4B with N395H, Y403H), and the residues of PDE5A were mutated to the corresponding residues of PDE4 (5NYY: PDE5A with A767N, Q775Y, W853Y). The experiment presented in Figure 3 shows that mutation of these residues altered the selectivity of PDEs toward cyclic nucleotides, as determined by the relative amount of each cyclic nucleotide required to inhibit the activity. The following results are observed: PDE5A gains affinity for cAMP and loses affinity for its natural substrate cGMP in 5NYY (compare panels A and B). PDE4B dramatically gains affinity for cGMP although surprisingly retains some affinity for cAMP in 4AQW (compare panels C and D). PDE4B dramatically gains affinity for cGMP but loses some affinity for cAMP in 4HH (compare panels C, E, and F). By changing two residues, the selectivity of PDE4B for cAMP versus cGMP is decreased about 600-fold, and by changing three residues, the selectivity of PDE5A for cGMP versus cAMP is decreased almost 600-fold. These results help validate the glutamine switch mechanism of nucleotide selectivity.

The glutamine switch mechanism proposed in this report also substantiates previously described site directed mutagenesis experiments that explored the roles of key residues predicted to control nucleotide specificity (Herman et al., 2000; Richter et al., 2001). Mutation of a relatively conserved aspartate (D241 in PDE4B2B, Supplemental Figure S1) to asparagine or alanine in PDE4A4, PDE4B1, and PDE4D3 significantly altered the substrate selectivity from cAMP-specific to dual cAMP and cGMP binding and hydrolysis. In our structure, D241 forms an H-bond network through a water with Y233 which in turn H-bonds to N395. This stabilizes the N395 in a conformation that forms bidentate H-bonds with cAMP. Thus, the D241N mutation could form a direct H-bond with N395 in an alternative conformation that

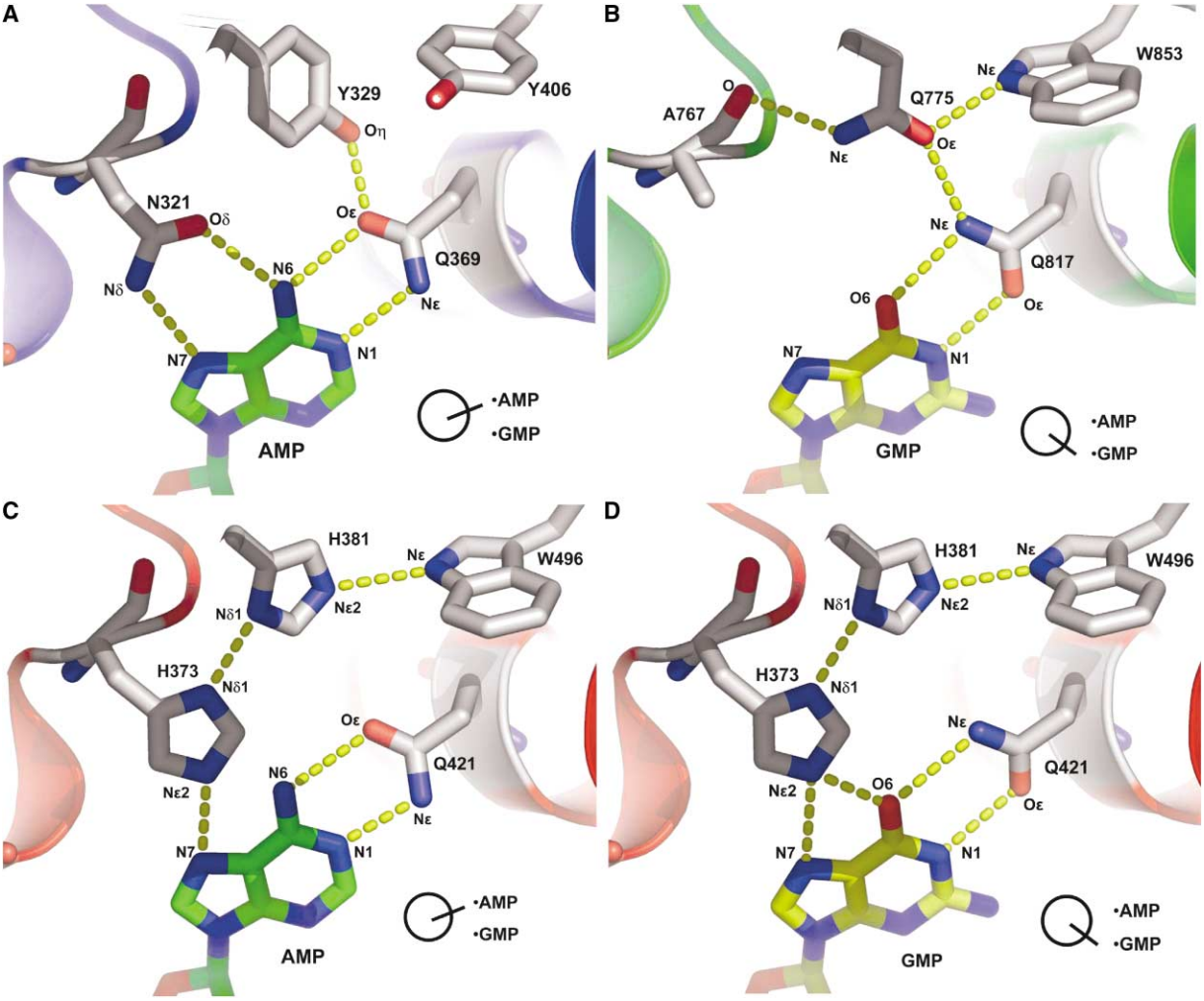

Figure 2. The Conserved Glutamine Is the Primary Selectivity Switch that Confers Nucleotide Specificity to PDEs

The protein ribbons for PDE1B, PDE4D, and PDE5A are represented by red, blue, and green, respectively. The ball-and-stick representation of protein side chains and nucleotides follows the same color scheme as in Figure 1. (A) Q369 recognizing AMP in PDE4D. Q369 forms a bidentate H-bond with the adenine moiety. Specifically, the Nϵ atom of Q369 donates an H-bond to the N1 atom of the adenine ring and the Oϵ accepts a H-bond from N6 in the exocyclic amino group of adenine. This particular orientation of Q369 is stabilized by H-bonding of Oϵ to the phenolic hydroxyl Oη of Y329. In addition, N321 forms a bidentate H-bond with the adenine base by donating one H-bond from Nδ to N7 of the adenine base and accepting one H-bond from the N6 of the exocyclic amino group to its Oδ. (B) Q817 recognizing GMP in PDE5A. Q817 forms a bidentate H-bond with GMP. The particular orientation of the Q817 side chain is anchored by its H-bond interaction with Q775. The orientation of Q775 side chain is in turn anchored by the H-bond between Nϵ in Q775 and the carbonyl oxygen in A767 and the H-bond between Oϵ of Q775 and the Nϵ of W853. (C) Q421 recognizing AMP in the model of AMP bound to PDE1B. (D) Q421 recognizing GMP in the model of GMP bound to PDE1B. In (C) and (D), there are no supporting residues to anchor the orientation of the key glutamine residue.

does not form H-bonds with either cAMP or cGMP, enabling non-selective binding and catalysis. Residues L192, F285, V302, A391 (the residue numbers have been converted to the PDE4B2B numbering from their respective PDE4 isoforms used in the experiment) are far away from the nucleotide binding site in our structure, consistent with the lack of influence on substrate affinity or specificity due to these residue mutations. By contrast, residues W176 and W406 are close to the nucleotide binding site, and their mutation is expected to disrupt the structural integrity of the binding site; mutations abolished catalytic activity. Residue P396 neighbors the N395 that forms bidentate H-bonds with cAMP, and hence could affect the ability of N395 to form bidentate H-bonds with cAMP; indeed P396 mutation decreased substrate affinity.

Conclusions

Precise modulation of PDE function in cells is critical for maintaining cyclic nucleotide levels within a narrow range of concentrations. Increases in cyclic nucleotides of 2- to 4-fold above the basal level will usually produce a maximum physiological response. In order to determine PDE activity, selection of either cAMP or cGMP and regulation of the catalytic efficiency must be precisely defined. The structural basis for the selectivity advances our understanding of PDE function.

The invariant glutamine residue forms essential hydro-

Table 1. Data Collection, Processing, and Refinement Statistics

Crystal	PDE1B	PDE4D + AMP	PDE4D + Rolipram	PDE4B + AMP	PDE5A	PDE5A + GMP	PDE5A + Sildenafil
Space Group	$P4_32_12$	$P2_12_12_1$	$P2_12_12_1$	$P2_12_12_1$	$P6_2$	$P2_1$	$P3_121$
Cell	87.232	60.316,	60.106,	89.547,	96.411,	61.969,	76.097,
(a,b,c,α,β,γ)	87.232	78.958,	79.019	94.241,	96.411,	90.872,	76.097,
	134.151	164.70,	164.548	107.243,	79.026,	68.991,	99.272,
	90,	90,	90,	90,	90,	90,	90,
	90,	90,	90,	90,	90,	98.07,	90,
	90	90	90	90	120	90	120
Resolution (Å)	1.77	1.63	1.60	2.15	2.1	2.0	1.3
Redundancy	8.9	2.9	3.5	4.7	10.9	3.8	6.5
Completeness (%)	99.8 (100)	92.6 (76.4)	93.0 (93.9)	99.9 (100)	99.5 (99.1)	100 (99.9)	99.6 (99.2)
I/σ(outer shell)	20.9(2.48)	9.0 (1.65)	9.5 (1.53)	9.2 (1.63)	8.2 (1.0)	6.4 (2.8)	12.2 (1.4)
R_{sym} (outer shell)	0.057 (0.703)	0.057 (0.590)	0.063 (0.758)	0.079 (0.751)	0.047 (0.696)	0.124 (0.558)	0.067 (0.803)
R_{work}/R_{free}	18.9/19.8	17.9/19.2	18.6/20.4	23.2/26.6	20.4/24.1	17.5/21.2	15.7/18.6
Number of Atoms	2816	5813	5878	5361	2559	5899	3021
RMSD bond (Å)	0.008	0.007	0.009	0.015	0.014	0.010	0.025
RMSD angle (°)	1.018	1.152	1.164	1.522	1.421	1.352	2.000
Ramachandra (core)	89.7	93.3	93.4	92.0	94.7	95.4	94.5
Ramachandra (allowed)	10.3	6.7	6.6	8.0	4.6	4.4	5.5
Ramachandra (generously)	0	0	0	0	0.7	0.2	0
Ramachandra (disallowed)	0	0	0	0	0	0	0

gen bonds to the purine ring. The specificity is then determined by neighboring residues that serve to orient the glutamine in the manner we describe as a selectivity switch. Two metal ions are bound to each of the PDE catalytic domains: tightly bound zinc and a second metal that is likely magnesium. In each of the structures reported here, these metal ions have octahedral coordination geometry. The zinc coordination sphere is made up of three histidines, an aspartate, and two water molecules, while the magnesium coordination sphere involves the same aspartate, and five water molecules, one of which is shared with the zinc. The putative roles of these metal ions include stabilization of the structure and activation of hydroxide to mediate catalysis.

In all co-crystal structures we have determined to date, which includes many known or new PDE inhibitors (data not shown), a central aromatic ring of the ligand is "clamped" by a pair of hydrophobic residues. This hydrophobic interaction provides much of the binding energy with these ligands. The structural understanding of nucleotide binding also aids in the design of specific PDE inhibitors. With the first direct comparison of nucle-

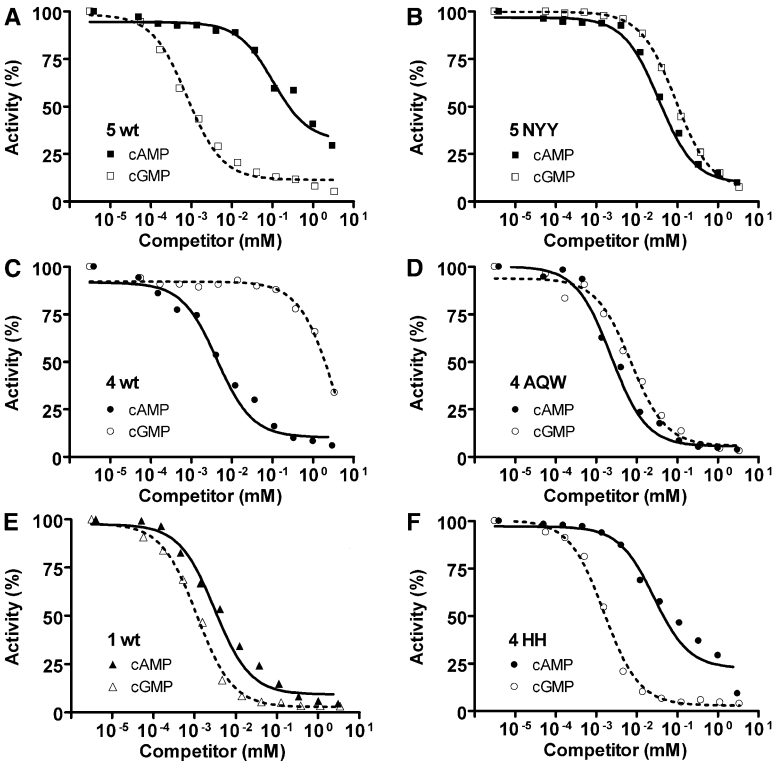

Figure 3. Mutations of PDE4B and PDE5A that Alter Selectivity of Competition by cAMP and cGMP

1wt, 4wt, and 5wt represent the wild-type catalytic domains of PDE1B, PDE4B, and PDE5A, respectively. 4HH is a double-mutation of PDE4B changing residue N395 to H and residue Y403 to H, thus matching the corresponding residues in PDE1B. 4AQW is a triple-mutation of PDE4B changing residues N395 to A, Y403 to Q, and Y480 to W, thus matching the corresponding residues in PDE5A. 5NYY is a triple-mutation of PDE5A changing residues A767 to N, Q775 to Y, and W853 to Y, thus matching the corresponding residues in PDE4B. Concentrations of each PDE protein were chosen to give 10% hydrolysis of 10 nM ^{3}H-cyclic nucleotide in 30 min (normalized to 100% on Activity scale), and the concentrations of cAMP (closed symbols) and cGMP (open symbols) required to inhibit hydrolysis were compared. (A) 5wt showed an obvious selectivity for cGMP. (B) 5NYY had a slight selectivity for cAMP. (C) 4wt showed an obvious selectivity for cAMP. (D) 4AQW retained a slight selectivity for cAMP. (E) 1wt showed slight selectivity for cGMP. (F) 4HH showed selectivity for cGMP. Results are representative of three experiments.

otide binding to different PDE family members we begin to understand what is common to ligand interactions within this important family and what regions of inhibitors or drugs are important for selectivity for individual PDE family members. These insights should facilitate the discovery of more potent and selective drugs for the treatment of a wide array of diseases.

Experimental Methods

Protein Expression and Purification

The cDNAs encoding the catalytic domains of human PDE1B (Jiang et al., 1996), PDE4B (McLaughlin et al., 1993), PDE4D (Bolger et al., 1993), and PDE5A (Loughney et al., 1998) were cloned into pET15b vectors (Novagen) in which a His-tag is appended to the coding sequence. In addition, a chimeric protein, in which residues R658-M681 from PDE5A were replaced by residues P279-L303 from PDE4B, was also subcloned into the pET15b expression vector. This protein will be referred to as PDE5A chimera. Numbering in the text refers to the wild-type PDE5A sequence (Loughney et al., 1998).

The proteins were expressed in *E. coli* [BL21(DE3)Codon Plus(-RIL); Novagen], cell pellets were lysed, and PDE proteins were purified initially through a metal affinity column and further purified by gel filtration and ion exchange chromatography. 100 μg/ml of lysozyme was added to the cell pellets and the cells were lysed in lysis buffer (0.1 M potassium phosphate buffer [pH 8.0], 10% glycerol, and 1 mM PMSF) in a Cell Disruptor (MircoFluidics). The clarified cell extract was bound to metal beads (Chelating Sepharose FF, Pharmacia), mixed at 4°C for 4 hr, and beads were washed in 0.1 M imidazole in lysis buffer, and eluted with 0.25 M imidazole in lysis buffer. The eluted protein was concentrated and separated on a Pharmacia Superdex 200 column (26/60) in low salt buffer (25 mM Tris-HCl [pH 8.0], 150 mM NaCl, and 14 mM beta-mercaptoethanol). Final purity was achieved by further chromatography on anion exchange columns (Source 30Q, Pharmacia) using a NaCl gradient.

Assay of Phosphodiesterase Activity

Measurement of phosphodiesterase activity takes advantage of the selective binding of 5′-AMP or 5′-GMP (and not cAMP or cGMP) to yttrium silicate beads with embedded scintillant. In brief, 0.1–1 nM PDE was incubated with 0.5 μCi/ml ^{3}H-cyclic nucleotide (Amersham, 5–60 Ci/mmol) in 50 mM Tris, 7.5, 8.3 mM $MgCl_2$, 1.7 mM EGTA, 0.01% BSA at 30°C for 30 min in 384-well assay plates. The assay was terminated by adding one-third volume of 5 mg/ml yttrium silicate beads in 18 mM ZnAcetate/$ZnSO_4$ solution (3:1). A minimum of 30 min after mixing and centrifuging the reaction, hydrolysis was quantified by reading in a scintillation counter (Trilux, Wallac).

Protein Crystallization, Data Collection, Structure Determination and Refinement

All proteins were crystallized using the sitting drop method. Crystals of PDE1B were grown in 50% MPD, 100 mM MES (pH 6.5), and 25 mg/ml protein at 4°C, using an Intelliplate (Robbins Scientific, Hampton) by mixing 1 μl of protein with 1 μl of precipitant, also at 4°C. Crystals of PDE4B with AMP were grown at 4°C by mixing equal volumes of the protein at 10 mg/ml with ammonium sulfate, buffered in a range 10.0–10.5, in the presence of lithium sulfate and 1 mM AMP. Crystals of PDE4D with AMP or Rolipram were grown at 15°C by mixing equal volumes of the protein at 30 mg/ml with a well buffer of polyethylene glycol (PEG) 3000, ethylene glycol, isopropanol, glycerol and DTT, and buffered in the range 6.0–8.5 and with compound concentration of 1 mM. Crystals of apo PDE5A were grown at 4°C by mixing equal volume of the protein at 8 mg/ml with a precipitant solution of PEG 3000, sodium chloride, and sodium phosphate-citrate buffered at pH 4.5. Crystals of PDE5A chimera in complex with GMP were grown at 4°C by mixing equal volume of the protein at 8 mg/ml with a precipitant solution of PEG 4000 and lithium sulfate buffered at pH 8.5 and 1 mM GMP. Crystals of PDE5A chimera and Sildenafil complex were grown at 4°C by mixing equal volume of the protein at 8 mg/ml with a precipitant solution of $(NH_4)_2SO_4$ and PEG 400 buffered at pH 7.5 and 1 mM Sildenafil.

X-ray diffraction data were collected at BL8.3.1 and BL5.0.1 of the Advanced Light Source (Lawrence Berkeley National Laboratory, Berkeley). The data was processed by Mosflm (Leslie, 1999) and Scala (Evans, 1993) driven by the ELVES (Holton and Alber, 2004) automation scripts.

The apo PDE5A crystal structure was solved by multiple-wavelength anomalous dispersion (MAD) method that takes advantage of the endogenous zinc ion bound to the enzyme. A three wavelength MAD dataset was collected to 2.5 Å resolution at the peak (9664.1 eV), the inflection point (9661.4 eV) of the zinc anomalous edge as well as at a high energy remote (10600.0 eV) using the inverse beam method. The identification of the anomalous scatter Zn and MAD phasing were performed using CNX (Brünger et al., 1998). The phasing power of a single zinc atom per protein molecule is 2.07 and the resulting phases have a figure of merit of 0.75. The map produced from the experimental phases is of superb quality and an initial model of the entire protein was easily built into this MAD phased map using O (Jones et al., 1991). This model was subsequently refined against a 2.1 Å native dataset to a final R factor of 20.4% and R-free of 24.1%.

The co-crystal structures of PDE4B, PDE4D and PDE5A chimera were solved by molecular replacement using EPMR (Kissinger et al., 1999) with the PDE4B apo structure (Xu et al., 2000) or the PDE4D apo structure (Huai et al., 2003b), or our PDE5A apo structure as search models, respectively. The structures were refined by CNX (Brünger et al., 1998) and REFMAC (Murshudov et al., 1999) with intermediate stages of manually rebuilding in O (Jones et al., 1991). The relevant data collection and refinement statistics are summarized in Table 1.

Acknowledgments

We thank Drs. Marco Conti and Axel Brünger for critical reading of this manuscript and discussions. We also thank Drs. Abhinav Kumar and Bruce England and our other colleagues at Plexxikon for help and discussion. We also thank the Advanced Light Source, which is supported by the Director, Office of Science, Office of Basic Energy Sciences, Materials Sciences Division, of the U.S. Department of Energy under Contract No. DE-AC03-76SF00098 at Lawrence Berkeley National Laboratory.

All the authors except Sung-Hou Kim and Joseph Schlessinger are employees of Plexxikon. Sung-Hou Kim and Joseph Schlessinger are co-founders of the company and shareholders of Plexxikon stock.

Received: March 10, 2004
Revised: May 14, 2004
Accepted: May 21, 2004
Published: July 22, 2004

References

Beavo, J.A., and Brunton, L.L. (2002). Cyclic nucleotide research—still expanding after half a century. Nat. Rev. Mol. Cell Biol. *3*, 710–718.

Bolger, G., Michaeli, T., Martins, T., St John, T., Steiner, B., Rodgers, L., Riggs, M., Wigler, M., and Ferguson, K. (1993). A family of human phosphodiesterases homologous to the dunce learning and memory gene product of Drosophila melanogaster are potential targets for antidepressant drugs. Mol. Cell. Biol. *13*, 6558–6571.

Brünger, A.T., Adams, P.D., Clore, G.M., DeLano, W.L., Gros, P., Grosse-Kunstleve, R.W., Jiang, J.S., Kuszewski, J., Nilges, M., Pannu, N.S., et al. (1998). Crystallography & NMR system: a new software suite for macromolecular structure determination. Acta Crystallogr. D Biol. Crystallogr. *54*, 905–921.

Conti, M. (2000). Phosphodiesterases and cyclic nucleotide signaling in endocrine cells. Mol. Endocrinol. *14*, 1317–1327.

Conti, M., Richter, W., Mehats, C., Livera, G., Park, J.Y., and Jin, C. (2003). Cyclic AMP-specific PDE4 phosphodiesterases as critical components of cyclic AMP signaling. J. Biol. Chem. *278*, 5493–5496.

Corbin, J.D., and Francis, S.H. (1999). Cyclic GMP phosphodiesterase-5: target of sildenafil. J. Biol. Chem. *274*, 13729–13732.

Evans, P.R. (1993). Data Reduction. Proceedings of CCP4 Study Weekend, On Data Collection and Processing, 114–122.

Herman, S.B., Juilfs, D.M., Fauman, E.B., Juneau, P., and Menetski, J.P. (2000). Analysis of a mutation in phosphodiesterase type 4 that alters both inhibitor activity and nucleotide selectivity. Mol. Pharmacol. *57*, 991–999.

Holton, J., and Alber, T. (2004). From the cover: automated protein crystal structure determination using ELVES. Proc. Natl. Acad. Sci. USA *101*, 1537–1542.

Houslay, M.D., and Adams, D.R. (2003). PDE4 cAMP phosphodiesterases: modular enzymes that orchestrate signalling cross-talk, desensitization and compartmentalization. Biochem. J. *370*, 1–18.

Huai, Q., Colicelli, J., and Ke, H. (2003a). The crystal structure of AMP-bound PDE4 suggests a mechanism for phosphodiesterase catalysis. Biochemistry *42*, 13220–13226.

Huai, Q., Wang, H., Sun, Y., Kim, H.Y., Liu, Y., and Ke, H. (2003b). Three-dimensional structures of PDE4D in complex with roliprams and implication on inhibitor selectivity. Structure (Camb) *11*, 865–873.

Huai, Q., Liu, Y., Francis, S. H., Corbin, J. D., and Ke, H. (2004). Crystal structures of phosphodiesterases 4 and 5 in complex with inhibitor IBMX suggest a conformation determinant of inhibitor selectivity. J Biol Chem. *279*, 13095–13101. Published online December 10, 2003.

Jiang, X., Li, J., Paskind, M., and Epstein, P.M. (1996). Inhibition of calmodulin-dependent phosphodiesterase induces apoptosis in human leukemic cells. Proc. Natl. Acad. Sci. USA *93*, 11236–11241.

Jones, T.A., Zou, J.Y., Cowan, S.W., and Kjeldgaard, M. (1991). Improved methods for building protein models in electron density maps and the location of errors in these models. Acta Crystallogr. *A47*, 110–119.

Kissinger, C.R., Gehlhaar, D.K., and Fogel, D.B. (1999). Rapid automated molecular replacement by evolutionary search. Acta Crystallogr. *D55*, 484–491.

Lee, M.E., Markowitz, J., Lee, J.O., and Lee, H. (2002). Crystal structure of phosphodiesterase 4D and inhibitor complex. FEBS Lett. *530*, 53–58.

Leslie, A.G. (1999). Integration of macromolecular diffraction data. Acta Crystallogr. D Biol. Crystallogr. *55*, 1696–1702.

Loughney, K., Hill, T.R., Florio, V.A., Uher, L., Rosman, G.J., Wolda, S.L., Jones, B.A., Howard, M.L., McAllister-Lucas, L.M., Sonnenburg, W.K., et al. (1998). Isolation and characterization of cDNAs encoding PDE5A, a human cGMP-binding, cGMP-specific 3′,5′-cyclic nucleotide phosphodiesterase. Gene *216*, 139–147.

McLaughlin, M.M., Cieslinski, L.B., Burman, M., Torphy, T.J., and Livi, G.P. (1993). A low-Km, rolipram-sensitive, cAMP-specific phosphodiesterase from human brain. Cloning and expression of cDNA, biochemical characterization of recombinant protein, and tissue distribution of mRNA. J. Biol. Chem. *268*, 6470–6476.

Mehats, C., Andersen, C.B., Filopanti, M., Jin, S.L., and Conti, M. (2002). Cyclic nucleotide phosphodiesterases and their role in endocrine cell signaling. Trends Endocrinol. Metab. *13*, 29–35.

Murshudov, G.N., Vagin, A.A., Lebedev, A., Wilson, K.S., and Dodson, E.J. (1999). Efficient anisotropic refinement of macromolecular structures using FFT. Acta Crystallogr. D Biol. Crystallogr. *55*, 247–255.

Pierce, K.L., Premont, R.T., and Lefkowitz, R.J. (2002). Seven-transmembrane receptors. Nat. Rev. Mol. Cell Biol. *3*, 639–650.

Richter, W., Unciuleac, L., Hermsdorf, T., Kronbach, T., and Dettmer, D. (2001). Identification of substrate specificity determinants in human cAMP-specific phosphodiesterase 4A by single-point mutagenesis. Cell. Signal. *13*, 159–167.

Sonnenburg, W.K., Seger, D., Kwak, K.S., Huang, J., Charbonneau, H., and Beavo, J.A. (1995). Identification of inhibitory and calmodulin-binding domains of the PDE1A1 and PDE1A2 calmodulin-stimulated cyclic nucleotide phosphodiesterases. J. Biol. Chem. *270*, 30989–31000.

Sung, B.J., Yeon Hwang, K., Ho Jeon, Y., Lee, J.I., Heo, Y.S., Hwan Kim, J., Moon, J., Min Yoon, J., Hyun, Y.L., Kim, E., et al. (2003). Structure of the catalytic domain of human phosphodiesterase 5 with bound drug molecules. Nature *425*, 98–102.

Xu, R.X., Hassell, A.M., Vanderwall, D., Lambert, M.H., Holmes, W.D., Luther, M.A., Rocque, W.J., Milburn, M.V., Zhao, Y., Ke, H., et al. (2000). Atomic structure of PDE4: insights into phosphodiesterase mechanism and specificity. Science *288*, 1822–1825.

Xu, R.X., Rocque, W.J., Lambert, M.H., Vanderwall, D.E., Luther, M.A., and Nolte, R.T. (2004). Crystal structures of the catalytic domain of phosphodiesterase 4B complexed with amp 8-br-AMP, and rolipram. J. Mol. Biol. *337*, 355–365.

Accession Numbers

The coordinates and structure factors of the PDE apo and co-crystal structures have been deposited with the Protein Data Bank with the PDB code of 1TAZ for apo PDE1B, 1TB5 for PDE4B with AMP, 1TB7 for PDE4D with AMP, 1TBB for PDE4D with Rolipram, 1T9R for apo PDE5A, 1T9S for PDE5A with GMP, and 1TBF for PDE5A with Sildenafil.